$E0$ decay from the first 0^+ state in ^{156}Dy and ^{160}Er

N. Blasi,[1] L. Atanasova,[2] D. Balabanski,[3] S. Das Gupta,[4,5,*] K. Gladinski,[6] L. Guerro,[4,5] S. Nardelli,[4,5] and A. Saltarelli[4,5]

[1]*INFN, Sezione di Milano, via Celoria 16, 20133 Milano, Italy*

[2]*Department of Medical Physics and Biophysics, Medical University, Sofia 1431, Bulgaria*

[3]*ELI-NP, Hora Hulubei National Institute of Physics and Nuclear Engineering, 077125 Magurele, Romania*

[4]*INFN - Sezione di Perugia, via A. Pascoli - 06123, Perugia, Italy*

[5]*Division of Physics, School of Science and Technology, Università di Camerino, via Madonna delle Carceri-62032, Camerino (MC), Italy*

[6]*Faculty of Physics, St. Kliment Ohridski University of Sofia, Bulgaria*

(Received 9 September 2014; published 21 October 2014)

Excited states in ^{160}Er and ^{156}Dy were populated via β^+/EC decay and were studied via conversion electrons and γ-ray spectroscopy at the Tandem Accelerator in the INFN Laboratori Nazionali del Sud in Catania, Italy. Conversion electrons were detected by a mini-orange spectrometer with a transmission energy window that ranged from 500 to 1000 keV for ^{160}Er and from 350 keV to 750 keV for ^{156}Dy. The $E0$ decays of the first excited state at 893 keV in ^{160}Er and at 676 keV in ^{156}Dy were observed, and $X(E0/E2)$ ratios of reduced transition probabilities were deduced. Furthermore, for both nuclei $E0$ admixtures in transitions from the lower members of the β and γ bands to the ground-state band were observed, and $X(E0/E2)$ values were deduced. The values of the $X(E0/E2)$ for the 0_2^+ decays are compared to IBA-1 calculations that use the full Hamiltonian in multipole expansion. Properties related to the nuclear shape seem to be sensitive to higher-order terms of the expansion.

DOI: 10.1103/PhysRevC.90.044317 PACS number(s): 23.20.Nx, 27.70.+q, 21.60.Fw

I. INTRODUCTION

The recently proposed analytical solution of the Bohr collective Hamiltonian at the critical point of shape phase transitions between spherical and axially deformed shapes, denoted as X(5) [1], have triggered a number of studies in the mass region of $Z = 50$–82 due to the evidence of nuclear collective structure evolutions from weakly to well deformed as a function of N, Z, and A. Typical signatures for a X(5) nucleus are the following: (i) The ratio of the energies of the 4_1^+ and the 2_1^+ states E_4^+/E_2^+ is equal to 2.91; (ii) the energy ratio of the 0_2^+ and 2_1^+ states E_0^+/E_2^+ is equal to 5.67; (iii) the ground state $B(E2; \mathrm{I} \rightarrow \mathrm{I\ to\ 2})$ values increase at a rate intermediate between vibrator and rotor. ^{152}Sm [2], ^{154}Gd [3], and ^{156}Dy [4] were indicated as possible candidates. The X(5) solution is obtained by choosing a square-well potential in the Bohr Hamiltonian and an infinite number of particles, which might be considered unrealistic, but critical point and shape coexistence can also be studied within algebraic approaches, such as the Interacting Boson Approximation (IBA), which incorporates a finite boson number. McCutchan *et al.* [5] showed that, within the IBA framework, energy spectra that satisfy the X(5) scheme do not correspond to the shape coexistence region for boson numbers smaller than 25. On the other hand, the critical point is expected to hardly be found in nature since the shape variation is a function of a discrete quantity, i.e., the nucleon number. Nevertheless a nucleus can be close enough to the critical point to exhibit the main signatures predicted by the model, and a large number of studies have searched for critical point nuclei in this mass region [6–8].

An additional test property for the critical point, besides the energy of the 0_2^+ state, would be the monopole strength $\rho^2(E0)$ to the ground state [9,10] since it is related to the nuclear shape. An overview over shape coexistence and excited 0^+ states can be found in Ref. [11] where strong $\rho^2(E0)$'s are indicated as fingerprints for the presence of shape coexistence. Unfortunately, the measure of $\rho^2(E0)$ requires the lifetime measurement of the 0_2^+ state, which is rarely populated with sufficient intensity. As an alternative the quantity $X(E0/E2)$, i.e., the ratio between $E0$ and $E2$ transition intensities that deexcite the 0_2^+ state, is commonly used, but it has the disadvantage of theoretically implying two distinct parameters in the $E2$ and in the $E0$ operators. The quadrupole strength parameter e^2 can be fixed with a fit on the ground-state band $B(E2)$ values, but usually there are only very few known $E0$ transitions [12], if not only one, or even none. Furthermore, the $X(E0/E2)$ value is a ratio between two quantities usually rather small where one is the inhibited $E0$ transition and the other is the $E2$ transition from the β- to the ground-state band.

Since the monopole operator is related to the nuclear shape, it could be treated in a consistent way together with the mean-square charge radius, isotope, and isomer shifts so that the same parameters could be used. This has been suggested by Zerguine *et al.* [13], who performed calculations over all isotopes in the $A \approx 150$–170 region from samarium to tungsten by using a multipole expansion of the IBA-1 Hamiltonian and by allowing only the quadrupole parameter to vary along each isotope chain to reproduce energy levels, isotope shifts, and $\rho^2(E0)$'s. Other authors, Chou *et al.* [14] and McCutchan *et al.* [15], performed extensive calculations in this region by using different approaches. All these calculations were applied to reproduce the $X(E0/E2)$ values in the light Yb isotopes in a recent paper [16]. It was found that none of them could reproduce isotope shifts and $X(E0/E2)$ values reasonably and it was suggested that terms in the Hamiltonian usually

[*]Present address: Saha Institute of Nuclear Physics, 1/AF Bidhannagar, Kolkata-700064, India.

TABLE I. Nuclei expected in the reaction ^{150}Sm(^{14}N,4n) at 72 MeV and their decay chains. All data are taken from Ref. [19]. Half-lives are indicated in brackets. Levels of ^{160}Er measured in this paper were populated via the decay of ^{160}Tm.

Nuclei produced in the reaction ^{150}Sm(^{14}N,4n) at 73 MeV	Relative production[a] (%)	β^+/EC	Decay chains	
^{161}Tm (30 min)	3	$\rightarrow$ ^{161}Er (3.2 h)	$\rightarrow$ ^{161}Ho(2.5 h)	$\rightarrow$ ^{161}Dy
^{161}Er (3.2 h)	1	$\rightarrow$ ^{161}Ho (2.5 h)	$\rightarrow$ ^{161}Dy	
^{160}Tm (9 min)	57	$\rightarrow$ ^{160}Er (28 h)	$\rightarrow$ ^{160}Ho (26 min)	$\rightarrow$ ^{160}Dy
^{160}Er (28 h)	11	$\rightarrow$ ^{160}Ho (26 min)	$\rightarrow$ ^{160}Dy	
^{159}Tm (9 min)	19	$\rightarrow$ ^{159}Er (36 min)	$\rightarrow$ ^{159}Ho (33 min)	$\rightarrow$ ^{159}Dy (144 d)
^{159}Er (36 min)	1	$\rightarrow$ ^{159}Ho (33 min)	$\rightarrow$ ^{159}Dy (144 d)	
^{157}Ho (12 min)	8	$\rightarrow$ ^{157}Dy (8 h)	$\rightarrow$ ^{157}Tb (71 y)	

[a]From PACE4 calculations [20].

neglected could play a role in reproducing fine properties as $X(E0/E2)$ values.

To verify this suggestion we extended the analysis to the Er and the Dy isotopes. In the Er isotopes, $X(E0/E2)$ values are known for ^{162}Er, ^{164}Er, and ^{166}Er [12,17]. The critical point is predicted to lie between ^{160}Er and ^{162}Er [15]. Since the $X(E0/E2)$ value for the 0_2^+ in ^{160}Er is not known, we performed a new measurement.

In the Dy isotopes, $X(E0/E2)$ values are known for all isotopes from ^{154}Dy to ^{162}Dy with the exception of ^{158}Dy, whose $0_2^+ \rightarrow 0_1^+$ transition coincides with another transition of the same band. ^{156}Dy has been indicated as an X(5) candidate [4], therefore one expects a strong $\rho^2(E0)$ and an intermediate $X(E0/E2)$ value for the 0_2^+ state of this nucleus [16]. A previous measurement [18] reports a value of 0.08(5). In order to reduce the error, we performed a new measurement. The experimental setup and results are described in Sec. II. In Sec. III, the IBA-1 calculations mentioned above were extended to describe isotope shifts for the nuclei from ^{152}Dy to ^{160}Dy and from ^{154}Er to ^{164}Er. $X(E0/E2)$ values were then calculated by using the same parameters and were compared to the experimental values. It turns out that isotope shifts and $X(E0/E2)$ values are strongly related and quite sensitive to nuclear shape variations but also sensitive to the choice of the Hamiltonian parameters. New calculations that use the full IBA-1 Hamiltonian are presented.

II. EXPERIMENTS

A. The reactions

1. ^{160}Er

The experiments were performed at the INFN Laboratori Nazionali del Sud (LNS) in Catania. Beams were provided by the LNS Tandem Accelerator.

Levels of ^{160}Er were populated by the EC decay of ^{160}Tm: ^{160}Tm (9.4 min) $\rightarrow$ ^{160}Er. The father nucleus ^{160}Tm was produced by the ^{150}Sm (^{14}N,4n) fusion evaporation reaction at $E_{\rm beam} = 72$ MeV. The self-supporting target was $\sim 0.6 - {\rm mg/cm^2}$ thick. The full decay chain is the following: ^{160}Tm (9.4 min) $\rightarrow$ ^{160}Er (28 h) $\rightarrow$ ^{160}Ho (25 min) $\rightarrow$ ^{160}Dy.

The decay of ^{160}Er does not produce γ transitions in ^{160}Ho [19], but from the last decay several transitions of ^{160}Dy are observed. A beam-pulsing device, which consists of a fast switching shutter, was used to irradiate the target at fixed intervals. In our case the on-off period was set to 10 min/10 min, and data were taken only during beam-off intervals. Other nuclei are populated in the reaction, and they are listed in Table I together with their decay chains. The relative intensities of the γ transitions populated in these nuclei via EC decay are all known, therefore it was possible to monitor possible contaminations in transitions of interest. Figures 1 and 2 show the recorded γ and electron spectra, respectively, in the energy region of interest.

2. ^{156}Dy

Levels of ^{156}Dy were populated by the EC decay of ^{156}Er: ^{156}Er (19.5 min) $\rightarrow$ ^{156}Ho (56 min) $\rightarrow$ ^{156}Dy. ^{156}Er was produced by the ^{148}Sm (^{12}C,4n) fusion evaporation reaction at $E_{\rm beam} = 72$ MeV. The self-supporting target was $\sim$0.8-mg/cm^2 thick. The decay of ^{156}Er produces only few low energy γ transitions in ^{156}Ho [19] and does not affect the ^{156}Dy spectrum. The on-off period of the switching shutter was set to 1 h/1 h, and data were taken during beam off. In this case, data were also recorded during beam on to normalize the transmission curve to known transitions in ^{156}Er as explained

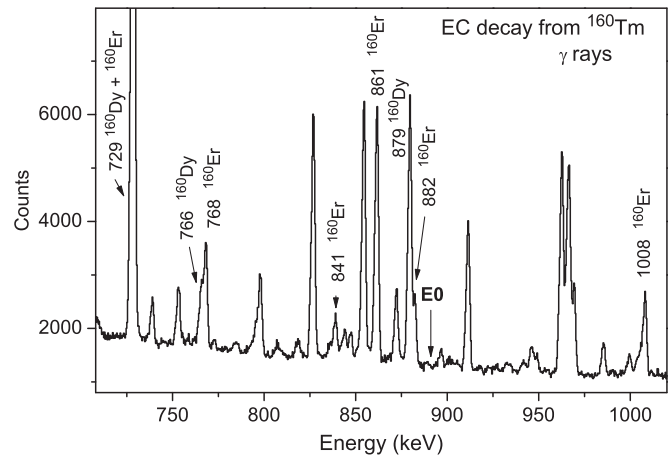

FIG. 1. The γ spectrum from the EC decay of ^{160}Tm populated via the ^{150}Sm(^{14}N,4n) reaction is shown. Transitions discussed in the text are indicated. The position that corresponds to the energy of the $E0$ transition is also indicated.

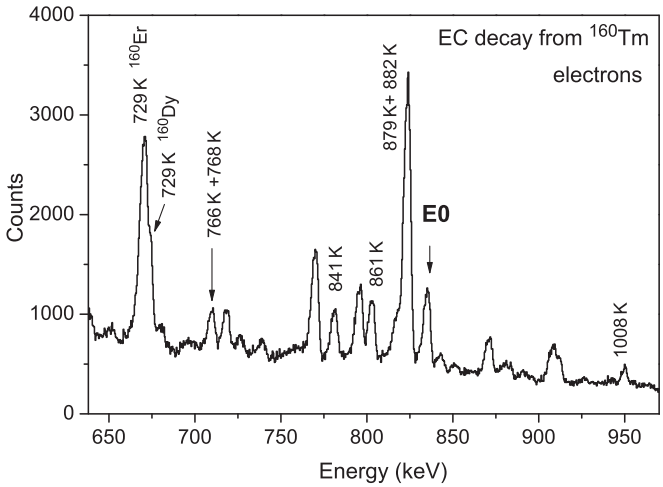

FIG. 2. The electron spectrum from the EC decay of ^{160}Tm populated via the ^{150}Sm(^{14}N,4n) reaction is shown. Transitions discussed in the text are indicated. The $E0$ transition is also indicated.

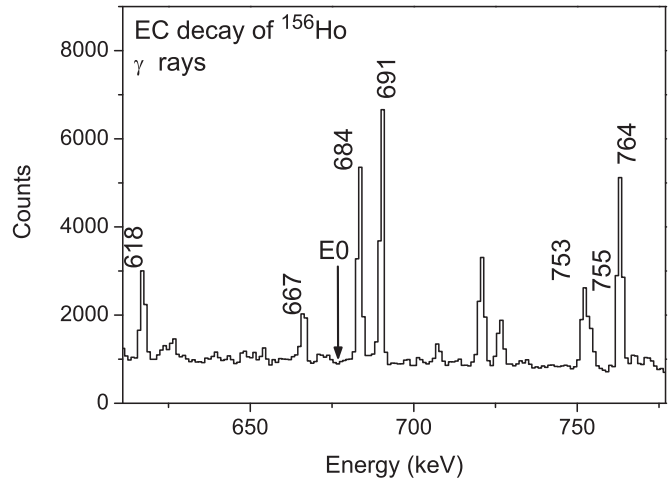

FIG. 3. The γ spectrum from the EC decay of ^{156}Ho populated via the ^{148}Sm(^{12}C,4n) reaction is shown. Transitions of ^{156}Dy discussed in text are indicated. The position that corresponds to the energy of the $E0$ transition is indicated.

in Sec. II C. Besides ^{156}Er, ^{156}Ho and ^{157}Er are produced in the reaction with non-negligible intensity. They are listed in Table II together with their decaying chains. In Figs. 3 and 4 the recorded γ and electron spectra, respectively, in the energy region of interest are shown.

B. The experimental setup

Internal conversion coefficients, defined as the ratio between electron and γ-emission rates, were determined by simultaneously measuring γ rays and conversion electrons. γ rays were recorded by a coaxial Compton suppressed HPGe detector, and conversion electrons were recorded by a mini-orange spectrometer (MOS) [21]. The coaxial HPGe detector, which has an energy resolution of 2.3 keV at 1332 keV, was positioned at 90° with respect to the beam direction. The MOS consists of a magnetic lens made of permanent magnets in front of a Si(Li) detector cooled to a liquid-nitrogen temperature. The MOS was placed at 45° with respect to the beam in the backward direction. The energy resolution of the MOS is entirely due to the properties of the silicon detector and was ≈7 keV. Since conversion coefficients are deduced from the ratio of the γ-ray and electron intensities, it is important to calibrate the efficiency of the detectors. The energy and efficiency calibrations of the HPGe detector were measured by using ^{152}Eu and ^{207}Bi sources placed in the target position. A further check was possible by using the known relative γ-ray intensities of nuclei populated in the experiment.

C. The MOS transmission curves

The magnetic field produced by the permanent magnets in the MOS has the only purpose of filtering and transporting the electrons to the detector. The efficiency of the apparatus is therefore strongly energy dependent. The position and the width of the transmission window depend on the type and number of magnets and on the distance between the magnets and the source and between the magnets and the silicon detector.

The 0_2^+ state lies at 894 keV in ^{160}Er and at 676 keV in ^{156}Dy. Therefore we choose two different transmission windows, the first that ranges approximately from 500 to 1000 keV and the second from 350 up to 750 keV.

The transmission curves have been measured by using the method of Ref. [22]: Energy spectra of the continuum β^- source ^{90}Sr were measured and were corrected for electron backscattering by using discrete sources (^{133}Ba,^{207}Bi). Transitions with known multipolarity and/or known internal conversion coefficients from levels populated in the EC decay were used as normalization for ^{160}Er, whereas for the ^{156}Dy transmission curve, transitions in ^{156}Er, measured in beam, were used. The resulting curves are shown in Figs. 5 and 6.

TABLE II. Nuclei expected in the reaction ^{148}Sm(^{12}C,4n) at 72 MeV and their decay chains. Data are taken from Ref. [19]. Half-lives are indicated in brackets. Levels of ^{156}Dy measured in this paper were populated via the decay of ^{156}Er and ^{156}Ho.

Nuclei produced in the reaction ^{148}Sm(^{12}C,4n) at 72 MeV	Relative production[a] (%)	β^+/EC	Decay chains	
^{157}Er (18 min)	7	→ ^{157}Ho (12 min)	→ ^{157}Dy (8 h)	→ ^{157}Tb (71 y)
^{156}Er (19 min)	77	→ ^{156}Ho (56 min)	→ ^{156}Dy	
^{156}Ho (56 min)	6	→ ^{156}Dy		

[a]From PACE4 calculations [20].

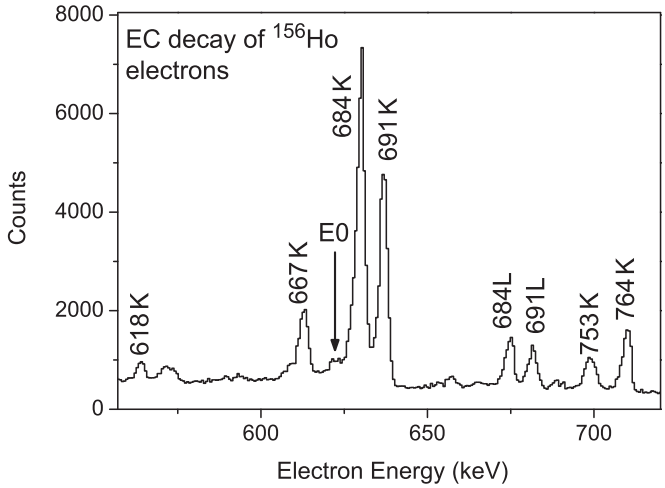

FIG. 4. The electron spectrum from the EC decay of ^{156}Ho populated via the ^{148}Sm(^{12}C,4n) reaction is shown. Transitions of ^{156}Dy discussed in text are indicated. The position of the $E0$ transition is also indicated.

D. Results and discussion

1. The E0 decay

For an $E0$ transition it is not possible to define an internal conversion coefficient since no γ transition is allowed. Usually, one defines [23] the dimensionless ratio of the $E0$ and $E2$ reduced transition probabilities $X(E0/E2) = \rho^2(E0)e^2R^4/B(E2)$ or the equivalent experimental value [12],

$$X(E0/E2) = 2.54 \times 10^9 A^{4/3} q_k^2 \left(\frac{E0}{E2}\right) \frac{\alpha_K(E2)}{\Omega_k(E0)} E_\gamma^5,$$

where $\alpha_K(E2)$ is the internal $E2$ conversion coefficient, $\Omega_k(E0)$ is the electronic factor, and $q_k^2(E0/E2)$ is the ratio between the $E0$ and the $E2$ K-electron intensities $I_k(E0)$ and $I_k(E2)$. In the case of a $0_2^+ \rightarrow 0_1^+$ transition, $E2$ refers to the $0_2^+ \rightarrow 2_1^+$ decay. The intensity of this $E2$ transition is not always strong enough to be observed in the electron spectrum. In this case it is still possible to deduce the $X(E0/E2)$ value. In fact, if the γ transition is observed or its intensity is known, one can calculate $I_k(E2)$ by using the theoretical $\alpha_K(E2)$ value. Another possibility is to refer to a well-known $E2$ transition other than the $0_2^+ \rightarrow 2_1^+$ one if the relative γ intensities I_γ are known

$$I_k(E2) = \frac{\alpha_K(E2)}{\alpha_K(E2')} \frac{I_\gamma(E2)}{I_\gamma(E2')} I_k(E2'),$$

where $E2'$ refers to the well-known transition.

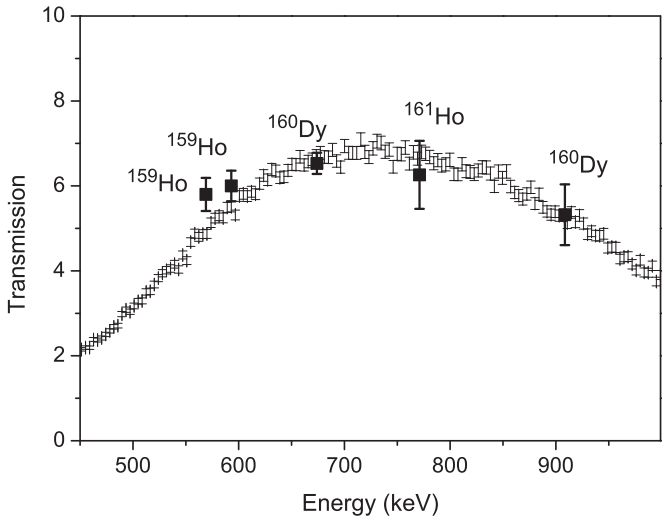

FIG. 5. The transmission curve used for the ^{150}Sm(^{14}N,4n) reaction is shown. The full square points refer to known transitions measured in the same reaction.

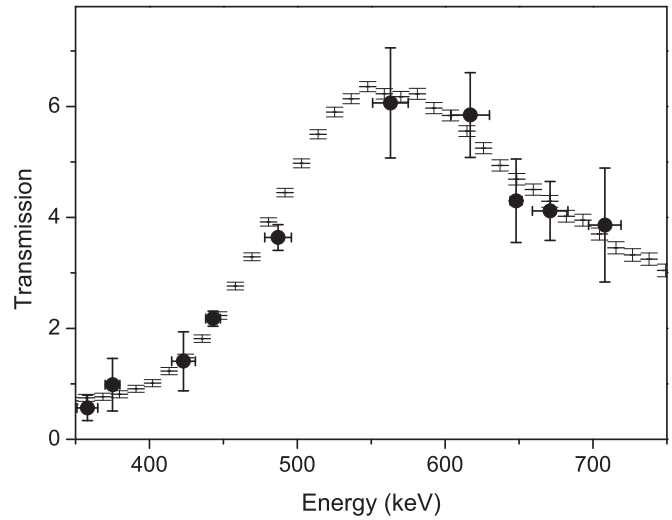

FIG. 6. The transmission curve for the ^{148}Sm(^{12}C,4n) reaction is shown. The points refer to ^{156}Er transitions with known multipolarity measured in beam. Large error bars are due to unresolved multiples.

2. E0 decay from the 0_2^+ state at 894 keV in ^{160}Er

A partial level scheme of ^{160}Er is shown in Fig. 7. The excited 0_2^+ level at 894 keV is known from EC decay [17]. In our γ spectrum no γ transition is observed at 894 keV as expected for an $E0$ transition (see Fig. 1). In the electron spectrum, shown in Fig. 2, the K transition that corresponds

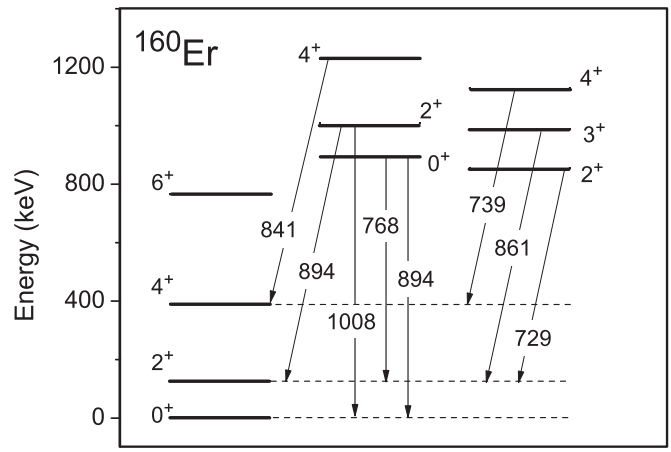

FIG. 7. Partial level scheme of ^{160}Er: The lower members of the ground-state, β, and γ bands are drawn.

to the $0_2^+ \rightarrow 0_1^+$ decay from the 894-keV level in ^{160}Er is observed. Note that no L- or M-electron transitions are expected at the same energy.

The $0_2^+ \rightarrow 2_1^+$ decay at 768 keV is also observed both in the γ and in the electron spectra, but it forms a doublet with the 766-keV transition of ^{160}Dy. In the γ spectrum, the energy difference is sufficient to disentangle the two contributions, but in the electron spectrum the energy difference of the two peaks decreases to 1 keV due to the difference in the electron binding energies, and we can only deal with the sum area. Nevertheless we can calculate the expected electron area from the γ intensity of the $E2$ transition by using the theoretical electron conversion coefficient $\alpha_K = 0.004\,87$ [24] and obtain the $X(E0/E2)$ value 0.11 (3). As an alternative, since the 766 transition in ^{160}Dy is a $3^+ \rightarrow 4^+$ $E2/M1$ decay with a known mixing ratio ($\delta = -13$) [17], we can also calculate the electron area for this transition and can subtract its contribution from the total doublet area by obtaining the area that corresponds to the $E2$ transition. In this case, the $X(E0/E2)$ value turns out to be 0.11 (3), in agreement with the previous result.

3. *E0 decay from the β-band members in* ^{160}Er

The 2^+ state at 1008 keV is considered to belong to the β band [17]. It deexcites via γ transitions to the ground state, to the 2_1^+ state, and to the 4_1^+ state. We observe all three transitions in the γ spectrum.

In the electron spectrum, the K transition to the ground state at 950 keV is observed, and the measured conversion coefficient is $\alpha_K = 0.0033\,(8)$, in good agreement with the expected $E2$ conversion coefficient [0.0028 (1)] [24]. The 882 keV γ transition to the 2_1^+ state forms a doublet with the $M1/E2$ transition at 879 keV, which belongs to ^{160}Dy, but it can be easily separated. In the electron spectrum the corresponding K transition at 824 keV differs only by 1 keV with the ^{160}Dy one. However, since the mixing ratio of the ^{160}Dy transition is known [$\delta = -16.6\,(5)$] [17], one can deduce the corresponding K-conversion coefficient [$\alpha_K = 0.003\,35$ (5)] and can calculate its contribution to the peak area. After subtraction of this contribution, one obtains the following value for the conversion coefficient of the $2_3^+ \rightarrow 2_1^+$ transition: $\alpha_K = 0.061$ (15). This value is much larger than what is expected for an $E2$ ($\alpha_K = 0.003\,63$) or a $M1$ ($\alpha_K = 0.0071$) transition, which indicates the presence of an $E0$ component.

The state at 1230 keV has been assigned spin and parity $I^\pi = 4^+$ by Dusling *et al.* [25], who placed this level in the β band. The state is populated in our experiment via the EC decay of the ^{160}Tm isomer with $I = 5$ and $T_{1/2} = 75$ s, and we observe both the $4^+ \rightarrow 2_1^+$ transition at 1104 keV and the $4^+ \rightarrow 4_1^+$ transition at 841 keV in the γ spectrum. In the electron spectrum, the acceptance window of the MOS leaves out the first one, but we do observe the K transition of the second one at 783 keV. The resulting conversion coefficient is $\alpha_K = 0.028\,(5)$, again much larger than what is expected for an $E2$ ($\alpha_K = 0.004\,02$) or a $M1$ ($\alpha_K = 0.0080$) transition. This indicates the presence of an $E0$ component, which supports the assignment of this state to the β band.

In Table III, the measured internal conversion coefficients are listed together with the deduced $X(E0/E2)$ values.

TABLE III. Electron conversion coefficients and $X(E0/E2)$ values for transitions in ^{160}Er.

	E_γ (keV)	E_e (keV)	$\alpha_K \times 1000$ This paper	$X(E0/E2)$ This paper
$2_\beta^+ \rightarrow 0_1^+$	1008	950	3.2 (7)	
$2_\beta^+ \rightarrow 2_1^+$	882	824	61 (15)	0.97 (21)
$4_\beta^+ \rightarrow 4_1^+$	841	783	28 (6)	0.330 (82)
$2_\gamma^+ \rightarrow 0_1^+$	854	797	4.0 (9)	
$2_\gamma^+ \rightarrow 2_1^+$	729	671	8.4 (14)	*0.023 (5)*[a]
$4_\gamma^+ \rightarrow 4_1^+$	739	681	6 (2)	0
$3_\gamma^+ \rightarrow 2_1^+$	861	804	3.8 (8)	

[a]This value is obtained by assuming an $E0+E2$ admixture with no $M1$ component.

4. *E0 decay from the γ-band members in* ^{160}Er

States of the γ band should not decay to the ground-state band via $E0$ transitions, unless a strong mixing with the β band is present.

The 2^+state at 854 keV is considered as the bandhead of the γ-vibrational band [17]. The state decays to the ground state and to the 2_1^+ state. For the 854-keV transition to the ground state we measure the conversion coefficient $\alpha_K = 0.0040$ (9), in good agreement with the expected $E2$ conversion coefficient [0.003 89 (6)] [24]. The transition to the 2_1^+ state at 729 keV overlaps with a strong $E2$ transition with the same energy that belongs to ^{160}Dy. Since the relative γ intensities are known, we may deduce that ^{160}Er contributes for 47% to the total peak area. The electron energies that correspond to these transitions are 671 keV for ^{160}Er and 674 keV for ^{160}Dy due to the different electron binding energies, and the peak can be fitted as a doublet. The conversion coefficient found for the $E2$ transition in ^{160}Dy is $\alpha_K = 0.0049$ (10), consistent with the reported value of $\alpha_K = 0.005\,03$ (6) [17]. The conversion coefficient for the $2_\gamma^+ \rightarrow 2_1^+$ transition in ^{160}Er turns out to be $\alpha_K = 0.0084$ (21). This value lies between the expected $E2$ [$\alpha_K = 0.005\,47$ (8)] and the $M1$ [$\alpha_K = 0.011\,40$ (16)] values, which correspond to a mixing ratio $\delta \approx 1$. However, in principle we cannot exclude the presence of a very small $E0$ component. In Table III the $X(E0/E2)$ value, deduced by assuming a $E0 + E2$ mixture, is given.

The state at 1129 keV has been assigned spin and parity $I^\pi = 4^+$ by Dusling *et al.* [25], who placed this level in the γ band. The state is known to decay only to the 4_1^+ state via the 739-keV transition. In our experiment it is populated via the EC decay of the ^{160}Tm isomer with $I = 5$ and $T_{1/2} = 75$ s, and we observe both the γ transition and the K-conversion electron peak at 681 keV. The deduced conversion coefficient is $\alpha_K = 0.006\,(2)$, consistent with the $E2/M1$ mixing ratio measured by Dusling *et al.* [25], $\delta = -7^{+3}_{-17}$, which corresponds to $\alpha_K = 0.005$ (6). This value would exclude the presence of an $E0$ component in this transition and confirms the assignment to the γ band.

Finally, we also measured the conversion coefficient of the decay of the 3_1^+ state at 987 keV to the 2_1^+ state. For this transition at 861 keV the value of $\alpha_K = 0.0034$ (8) found in

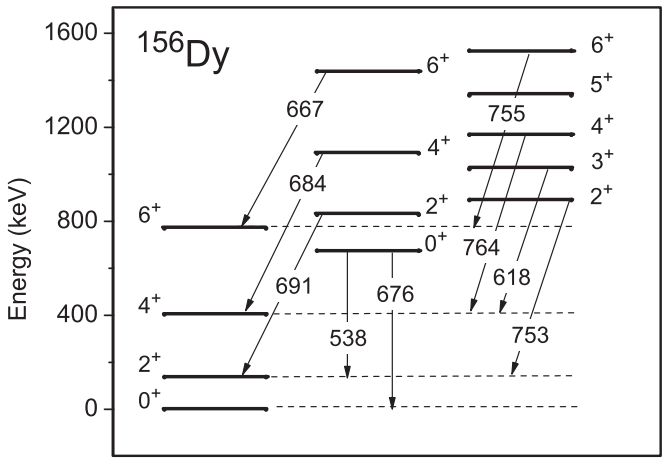

FIG. 8. Partial level scheme of ^{156}Dy: the ground-state, β, and γ bands up to $J^\pi = 6^+$ are drawn.

this paper is consistent with an $E2$ transition ($\alpha_K = 0.003\,82$ (6) [24]).

The measured internal conversion coefficients are summarized in Table III.

5. *E0 decay in* ^{156}Dy

A partial level scheme of ^{156}Dy is shown in Fig. 8. The 0_2^+ state is known to lie at 676 keV [17]. The $X(E0/E2)$ value of 0.08 (5) has previously been measured by Gromov *et al.* [18]. In our experiment, the electron conversion peak that corresponds to the $0_2^+ \rightarrow 0_1^+$ decay is observed at 622 keV. The $0_2^+ \rightarrow 2_1^+$ transition at 538 keV is observed both in the γ and in the electron spectra, and the measured K-conversion coefficient is $\alpha_K = 0.0106$ (60), in good agreement with the expected $E2$ value of $\alpha_K = 0.0102$ (20) [24]. The resulting $X(E0/E2)$ value is 0.061 (11). This value lies within the error bars of the one reported by Gromov *et al.* [18], and we reduce the uncertainty by a factor of 5. Also, we observe the $E0$ components in the transitions of the lower excited band members to the ground-state band up to $I^\pi = 6^+$. Conversion coefficients α_K and $X(E0/E2)$ values are listed in Table IV. These were previously measured by de Boer *et al.* [26] by

TABLE IV. Electron conversion coefficients and $X(E0/E2)$ values for transitions in ^{156}Dy.

	E_γ (keV)	E_e (keV)	$\alpha_K \times 1000$ This paper	$X(E0/E2)$ This paper
$2_\beta^+ \rightarrow 0_1^+$	538	484	10.6 (34)	
$2_\beta^+ \rightarrow 2_1^+$	691	637	36.4 (57)	0.25 (5)
$4_\beta^+ \rightarrow 4_1^+$	684	630	43.9 (69)	0.30 (5)
$6_\beta^+ \rightarrow 6_1^+$	667	613	46.8 (83)	0.29 (6)
$2_\gamma^+ \rightarrow 2_1^+$	753	699	16.8 (21)	0.14 (2)
$3_\gamma^+ \rightarrow 4_1^+$	618	564	8.4 (18)	
$4_\gamma^+ \rightarrow 4_1^+$	764	710	18.7 (21)	0.17 (3)
$6_\gamma^+ \rightarrow 6_1^+$	755	701	16.1 (20)	0.13 (2)

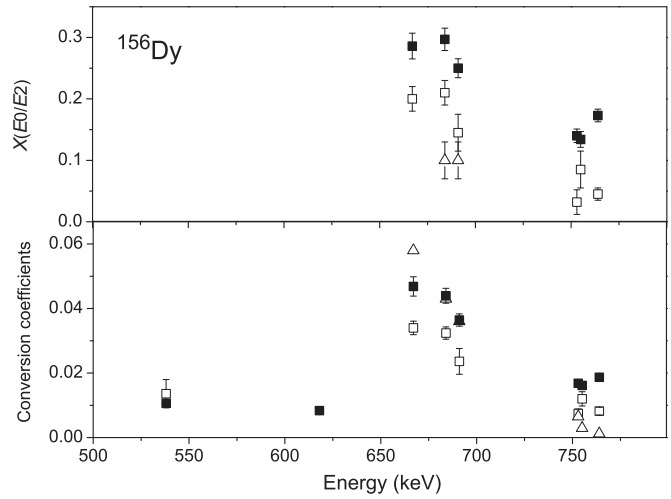

FIG. 9. Internal coefficients (bottom panel) and $X(E0/E2)$ values (upper panel) for ^{156}Dy obtained in this paper (full squares) are compared with the values of Ref. [26] (open squares) and Ref. [18] (open triangles).

populating ^{156}Dy with two fusion evaporation reactions and the EC decay of ^{156}Ho. It was found that not only the β band members decay to the ground state via strong $E0$, but also a non-negligible $E0$ contribution is unusually present in transitions from the γ band, which indicates a strong mixing between the β and the γ bands. In the bottom panel of Fig. 9 we compare the conversion coefficients deduced in this paper with the average values and the values obtained in the decay of ^{156}Ho of Ref. [26] and the values reported in Ref. [18]. In general our results are ≈30% larger than the previous ones, and the strong mixing between the β and the γ bands is confirmed. $X(E0/E2)$ values were calculated by assuming only $E2$ without any $M1$ admixture. They are compared with the values of Refs. [26,18] in the upper panel of Fig. 9.

Finally, we also measured the conversion coefficient of the decay of the 3_1^+ state at 1022 keV to the 4_1^+ state. For this transition at 618 keV the value of $\alpha_K = 0.0084$ (18) found in this paper is consistent with an $E2$ transition ($\alpha_K = 0.0073$ (1) [24]).

III. IBA-1 CALCULATIONS

Nuclear properties, such as strong $E0$ transitions, changes in isotope and isomer shifts, related to mean-square radii, or changes in two-nucleon separation energies, related to masses, can be regarded as fingerprints for shape coexistence [11]. In the mass region $A \sim 150$, $\rho^2(E0)$'s are known only for the Gd isotopes: The value is very small for the spherical ^{146}Gd, and it raises up to a maximum for ^{154}Gd, which well approximates X(5) and decreases for heavier isotopes. On the other hand, the $B(E2; 0_2^+ \rightarrow 2_1^+)$ value is large for spherical Gd nuclei and decreases with increasing deformation in such a way that the ratio $X(E0/E2)$ is close to zero for spherical nuclei, and it increases with increasing deformation until a maximum when deformation is well settled and then decreases again as can be seen in the upper panel of Fig. 10. There is therefore an indication that the critical point lies in the intermediate region

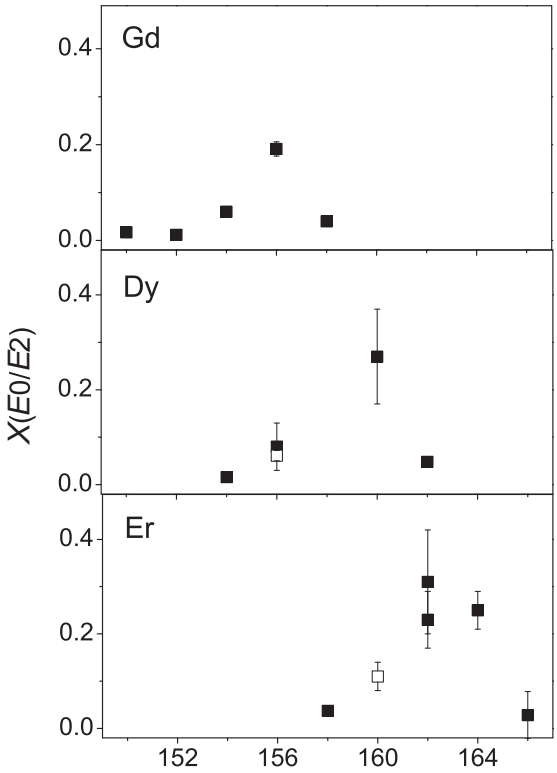

FIG. 10. Known $X(E0/E2)$ values for the Gd (top), Dy (middle), and Er (bottom) isotopes are shown with full squares. Data are from Refs. [12,16], and the open squares of ^{156}Dy and ^{160}Er are the present data. $X(E0/E2)$ is close to zero in spherical nuclei, and it increases with deformation by reaching a maximum in deformed nuclei and then decreases again. ^{154}Gd and ^{156}Dy are good X(5) candidates [3,4].

between the minimum $X(E0/E2)$ value on the spherical side and the maximum on the deformed side of the isotope chain.

The trend in the $X(E0/E2)$ values is similar for the other isotope chains in the region as shown in Fig. 10. For the Dy isotopes, the X(5) candidate is ^{156}Dy, whereas in the case of Er, the critical point seems to lie between ^{160}Er and ^{162}Er [6]: ^{160}Er is in fact closer to the spherical limit, and ^{162}Er is closer to the rotational one.

Recently, Zerguine *et al.* [13] suggested a relation between the mean-square charge radius $\hat{T}(r^2)$ and the monopole $\widehat{T}(E0)$ operators. More precisely, they derived the following expressions:

$$\hat{T}(r^2) = \langle r^2 \rangle_c + \alpha N_b + \eta \hat{n}_d,$$

$$\widehat{T}(E0) = (e_n N + e_p Z)\eta \hat{n}_d,$$

where $r^2{}_c$ is the charge radius of the core nucleus. Its contribution disappears when calculating isotope shifts. In fact, isotope shifts are given by the expression,

$$\Delta\langle r^2 \rangle^A = \langle r^2 \rangle^{A+2}_{\text{g.s.}} - \langle r^2 \rangle^{A}_{\text{g.s.}} = \alpha + \eta\left(\langle \hat{n}_d \rangle^{A+2}_{\text{g.s.}} - \langle \hat{n}_d \rangle^{A}_{\text{g.s.}}\right).$$

The authors also estimated that the parameter α, related to the dimension of the nucleus, should have a value on the order of $\approx 0.2\,\text{fm}^2$ in this mass region, whereas η, associated with

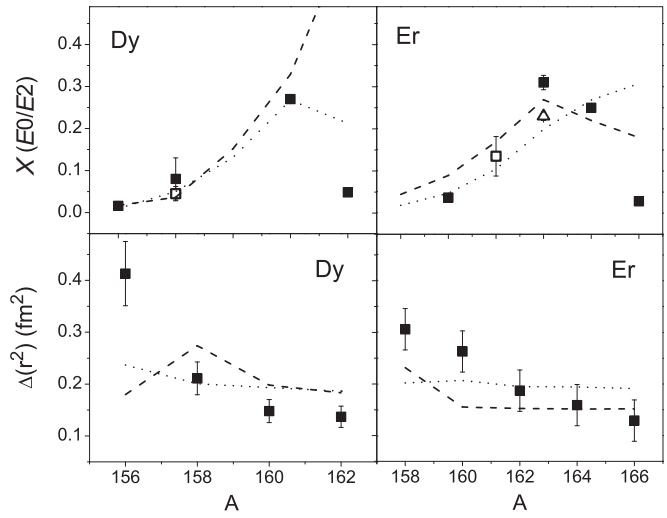

FIG. 11. Dy (left) and Er (right) isotope shifts (bottom) and $X(E0/E2)$ values (top) calculated by using the parameters of Chou *et al.* [14] (dashed line) and McCutchan *et al.* [15] (dotted line) are compared with the experimental ones (scatter points). Data represented by full squares are from Ref. [27], the open triangle is from Ref. [16], and the open square is from this paper.

the deformation contribution, should vary from $\approx$0.02 to $\approx$ 0.07 fm^2 from weakly deformed to strongly deformed nuclei.

Extensive calculations over all isotopes in the $A \approx$150–170 region from samarium to tungsten were performed by using a multipole expansion of the IBA-1 Hamiltonian and by allowing only the quadrupole parameter to vary along each isotope chain to fit energy spectra. They then applied the calculations to describe isotope shifts and $\rho^2(E0)$ where known. For the effective charges in the monopole operator, the authors found from a fit on charge radii that a reasonable choice was $e_p = e$ and $e_n = 0.5\,e$. The strict requirement on the parameters went to the detriment of the quality of the fit for the single nuclei.

Other extensive calculations were performed in the past in this mass region with the aim of describing the whole region with a small number of smoothly varying parameters by choosing a simplified Hamiltonian (extended consistent Q formalism) and by restricting the free parameters [14,15]. However, from a detailed analysis on light Yb isotopes [16] it was found that isotope shifts and $X(E0/E2)$ values are much more sensitive to the Hamiltonian parameters than energy levels or $B(E2)$ values, and the need to use the full Hamiltonian with a smooth variation of the parameters was suggested.

In the case of the Dy and Er isotopes, the calculations of Chou *et al.* [14] and McCutchan *et al.* [15] are in better agreement with the experimental isotope shifts and $X(E0/E2)$ values than for the Yb isotopes [16] as can be seen in Fig. 11. Nevertheless, the calculations of Chou *et al.* fail to reproduce the trend of the $X(E0/E2)$ values in ^{162}Dy, and the isotope shifts trend is always rather flat, whereas the calculations of McCutchan *et al.* fail to reproduce the trend of the $X(E0/E2)$ values in ^{166}Er and the trend of the isotope shifts in the lighter Dy isotopes and in the heavier Er isotopes. The values of parameters α and η used by Chou *et al.* were 0.12 and 0.065 for Dy and 0.15 and 0.06 for Er, respectively; McCutchan

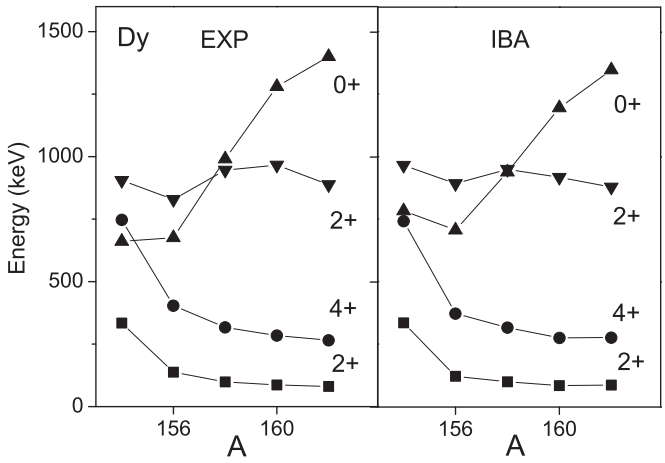

FIG. 12. Comparison between experimental (left) and calculated (right) 2_1^+, 4_1^+, 0_2^+, and 2_2^+ states of the Dy isotopes. The calculations are performed with a general IBA-1 Hamiltonian with parameters shown in Fig. 14.

et al. used 0.12 and 0.07 for Dy and 0.13 and 0.06 for Er, respectively.

By using the calculations of McCutchan *et al.* [15] as a starting point, we performed a new calculation for the Dy and Er isotopes by using the most general Hamiltonian as was used by Zerguine *et al.* [13] but by varying all the parameters with the only requirement of a smooth variation to simultaneously reproduce the yrast state energies and $B(E2)$ values, the β- and γ-bandhead energies, and the isotope shifts. Energy levels were reproduced reasonably well as can be seen in Figs. 12 and 13 where the experimental energies of the 2_1^+, 4_1^+, 2_γ^+, and 0_β^+ states are compared to the calculated ones. The resulting parameters are shown in Figs. 14 and 15.

The trend of the parameters for the two isotope chains turns out to be similar. Ground-state $B(E2)$ values (not shown) were reproduced by using a quadrupole strength parameter $e^2 = 0.15\ e$ b, kept constant for all isotopes. The effective

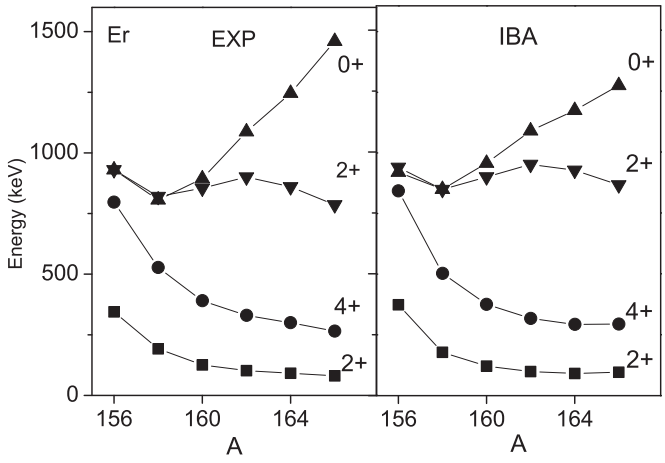

FIG. 13. Comparison between experimental (left) and calculated (right) 2_1^+, 4_1^+, 0_2^+, and 2_2^+ states of the Er isotopes. The calculations are performed with a general IBA-1 Hamiltonian with parameters shown in Fig. 15.

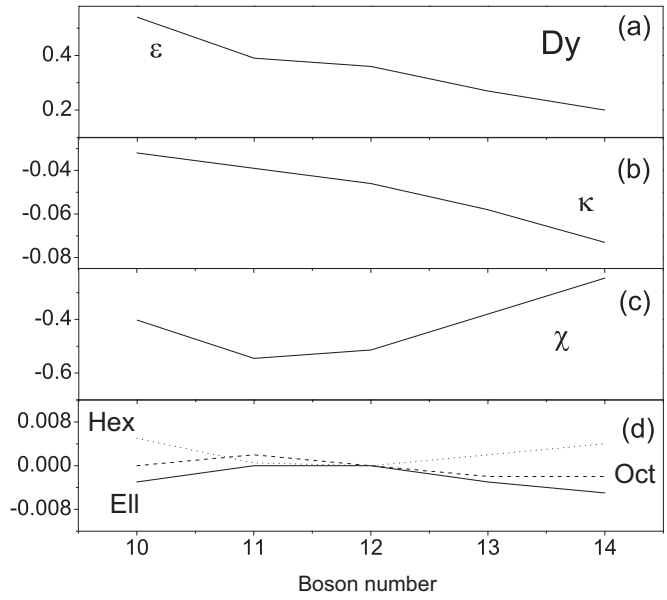

FIG. 14. Variation in the parameters of the general IBA-1 Hamiltonian as a function of boson number N_B for the Dy isotopes. N_B varies from 10 for ^{154}Dy to 14 for ^{162}Dy. (a) Parameters ε (monopole term), (b) κ (quadrupole term), (c) parameter χ (in the quadrupole term), and (d) ell, oct, and hex are the parameters of the (LL), octupole, and hexadecapole operators, respectively. All parameters are in MeV, except for χ, which is dimensionless.

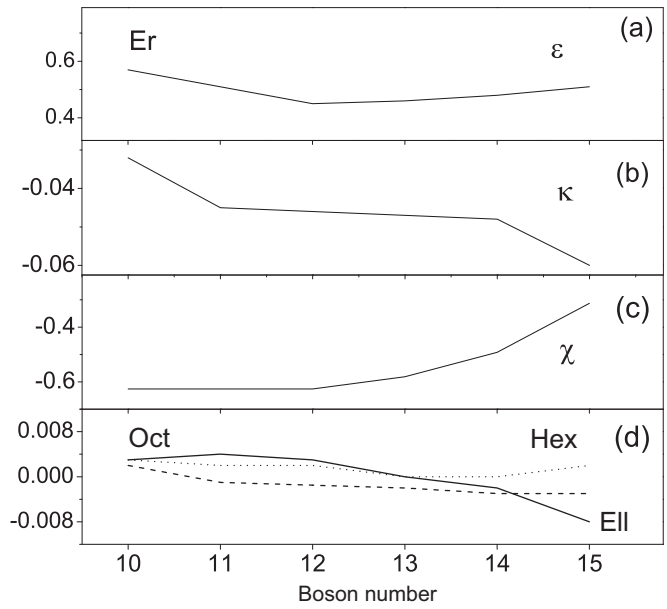

FIG. 15. Variation in the parameters of the general IBA-1 Hamiltonian as a function of boson number N_B for the Er isotopes. N_B varies from 10 for ^{156}Er to 15 for ^{166}Er. (a) Parameters ε (monopole term), (b) κ (quadrupole term), (c) parameter χ (in the quadrupole term), and (d) ell, oct, and hex are the parameters of the (LL), octupole, and hexadecapole operators, respectively. All parameters are in MeV, except for χ, which is dimensionless.

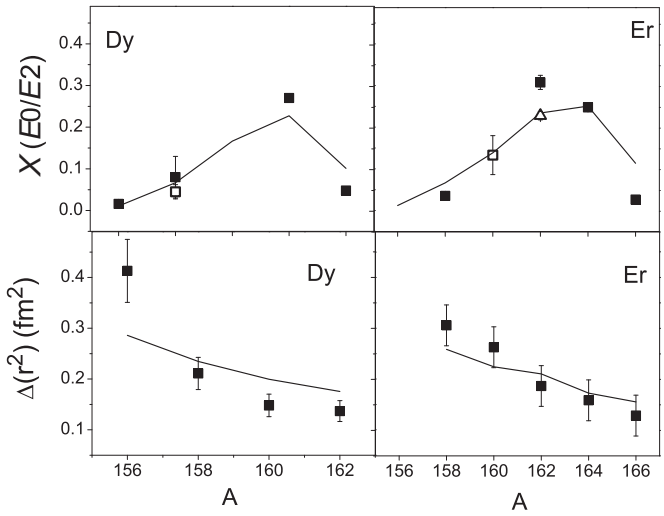

FIG. 16. Calculated isotope shifts (bottom) and $X(E0/E2)$ values (top) for the Dy (left) and Er (right) isotopes are compared with the experimental ones (full circles). The calculations are performed by using a general IBA-1 Hamiltonian with the parameters shown in Fig. 14 (Dy) and Fig. 15 (Er). Data are from Ref. [26]. $\alpha = 0.145$ and $\eta = 0.065$ for Dy and $\alpha = 0.17$ and $\eta = 0.065$ for Er.

charges in the expression of the $E0$ operator were $e_n = 0.5$ and $e_p = 1$ as suggested in Ref. [13]. Isotope shifts, fitted by using the parameters $\alpha = 0.145$ and $\eta = 0.065$ fm^2 for Dy and $\alpha = 0.170$ and $\eta = 0.065$ fm^2 for Er, are shown in the lower panels of Fig. 16. $X(E0/E2)$ values were then calculated with no further free parameter, and the results are shown in the upper panels of Fig. 16. The values of parameters α and η are in good agreement with the values estimated in Ref. [13]. The overall agreement is rather good. It is evident that both isotope shifts and $X(E0/E2)$ values are quantities quite sensitive to a fine-tuning of the parameters. In particular, the $E0$ strength appears to be sensitive mostly to the hexadecapole term $(d^+\tilde{d})^{(4)}$ in the Hamiltonian among the usually neglected terms.

IV. CONCLUSIONS

We measured the conversion electrons for the $E0$ transitions $0_2^+ \rightarrow 0_1^+$ in ^{160}Er and ^{156}Dy by using a MOS. γ rays were measured simultaneously with a high-resolution HPGe detector. To reduce the experimental uncertainty, special care was taken in determining the transmission curve of the MOS by using the method outlined in Ref. [22]. The $X(E0/E2)$ values of 0.11 (3) and 0.061 (11) were obtained for ^{160}Er and ^{156}Dy, respectively. In the same experiment, other $E0$ transitions between members of the β or γ bands and the ground state were observed. Conversion coefficients for transitions from the β and γ bands to the ground-state band were also measured.

We extended the analysis outlined in Ref. [16] to the Dy and Er isotopes by applying the IBA-1 model to reproduce $X(E0/E2)$ values by starting from the suggestion of Zerguine *et al.* [13] of relating the mean-square charge radius and the monopole operators. We applied it to IBA-1 calculations available in literature [13–15] in this mass region to calculate $X(E0/E2)$ values. From the results one may conclude that, although gross nuclear features, such as energies and large $B(E2)$ values, can be easily reproduced by calculations that use several different simplified approaches within the IBA-1 formalism, properties related to the nuclear shape, such as $E0$ transitions or isotope shifts, are much more sensitive and discriminating. In fact, a small variation in the parameters of the Hamiltonian, which does not affect the quality of the fit on energy levels, produces large changes in features related to the nuclear shape. We also performed a new calculation on the Er and Dy isotopes by using the full IBA-1 Hamiltonian by varying all the parameters with the only requirement of a smooth variation to simultaneously reproduce the yrast state energies and $B(E2)$ values, the β- and γ-bandhead energies, and the isotope shifts. We obtained good agreement for energies and $B(E2)$ values and an improved description of the isotope shifts. The resulting $X(E0/E2)$ values, obtained with no further free parameter, are in rather good agreement with the experimental values.

[1] F. Iachello, Phys. Rev. Lett. **87**, 052502 (2001).
[2] R. F. Casten and N. V. Zamfir, Phys. Rev. Lett. **87**, 052503 (2001).
[3] D. Tonev, A. Dewald, T. Klug, P. Petkov, J. Jolie, A. Fitzler, O. Moller, S. Heinze, P. von Brentano, and R. F. Casten, Phys. Rev. C **69**, 034334 (2004).
[4] M. A. Caprio, N. V. Zamfir, R. F. Casten, C. J. Barton, C. W. Beausang, J. R. Cooper, A. A. Hecht, R. Krucken, H. Newman, J. R. Novak, N. Pietralla, A. Wolf, and K. E. Zyromski, Phys. Rev. C **66**, 054310 (2002).
[5] E. A. McCutchan, N. V. Zamfir, and R. F. Casten, Phys. Rev. C **71**, 034309 (2005).
[6] R. M. Clark, M. Cromaz, M. A. Delaplanque, M. Descovich, R. M. Diamond, P. Fallon, R. B. Firestone, I. Y. Lee, A. O. Macchiavelli, H. Mahmud, E. Rodriguez-Vieitez, F. S. Stephens, and D. Ward, Phys. Rev. C **68**, 037301 (2003).
[7] E. A. McCutchan, N. V. Zamfir, M. A. Caprio, R. F. Casten, H. Amro, C. W. Beausang, D. S. Brenner, A. A. Hecht, C. Hutter, S. D. Langdown, D. A. Meyer, P. H. Regan, J. J. Ressler, and A. D. Yamamoto, Phys. Rev. C **69**, 024308 (2004).
[8] P. Cejnar, J. Jolie, and R. F.Casten, Rev. Mod. Phys. **82**, 2155 (2010).
[9] P. von Brentano, V. Werner, R. F. Casten, C. Scholl, E. A. McCutchan, R. Krücken, and J. Jolie, Phys. Rev. Lett. **93**, 152502 (2004).
[10] J. Bonnet, A. Krugmann, J. Beller, N. Pietralla, and R. V. Jolos, Phys. Rev. C **79**, 034307 (2009).
[11] K. Heyde and J. L. Wood, Rev. Mod. Phys. **83**, 1467 (2011).
[12] T. Kibedy and R. H. Spear, At. Data Nucl. Data Tables **89**, 77 (2005).
[13] S. Zerguine, P. Van Isacker, and A. Bouldjedri, Phys. Rev. C **85**, 034331 (2012).

[14] W. T. Chou, N. V. Zamfir, and R. F. Casten, Phys. Rev. C **56**, 829 (1997).
[15] E. A. McCutchan, N. V. Zamfir, and R. F. Casten, Phys. Rev. C **69**, 064306 (2004).
[16] N. Blasi, L. Guerro, A. Saltarelli, O. Wieland, and L. Fortunato, Phys. Rev. C **88**, 014318 (2013).
[17] ENSDF, http://www.nndc.bnl.gov/ensdf/
[18] K. Y. Gromov, Z. T. Zhelev, K. Zuber, Y. Zuber, T. Islamov, V. V. Kuznetsov, H.-G. Ortlepp, A. V. Potempa, Acta Phys. Pol., B **7**, 507 (1976).
[19] Table of radioactive isotopes, http://ie.lbl.gov/toi/
[20] Code PACE4, http://lise.nscl.msu.edu/pace4.html
[21] J. van Klinken, S. J. Feenstra, and G. Dumont, Nucl. Instrum. Methods **151**, 433 (1978).
[22] L. Guerro, N. Blasi, and A. Saltarelli, Nucl. Instrum. Methods Phys. Res., Sect. A **739**, 32 (2014).
[23] J. O. Rasmussen, Nucl. Phys. **19**, 85 (1960).
[24] http://bricc.anu.edu.au/
[25] K. Dusling, N. Pietralla, G. Rainovski, T. Ahn, B. Bochev, A. Costin, T. Koike, T. C. Li, A. Linnemann, S. Pontillo, and C. Vaman, Phys. Rev. C **73**, 014317 (2006).
[26] F.W. N. de Boer, P. Koldewijn. R. Beetz, J. L. Maarleveld, J. Konijn, R. Janssens, and J. Vervier, Nucl. Phys. A **290**, 173 (1977).
[27] E. Otten, in *Treatise on Heavy-Ion Science. VIII Nuclei Far From Stability*, edited by D. A. Bromley (Plenum, New York, 1989), p. 517.